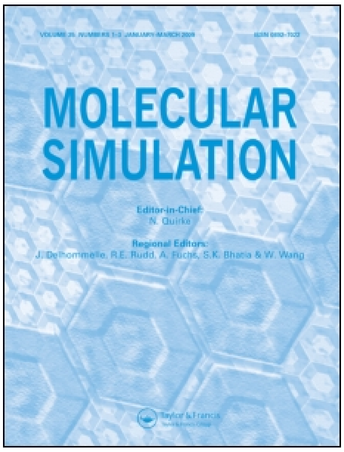

**Molecular Simulation**
Publication details, including instructions for authors and subscription information:
http://www.informaworld.com/smpp/title~content=t713644482

# A theoretical study of cooperative and anticooperative effects on hydrogen-bonded clusters of water and the cyanuric acid

Abedien Zabardasti[a]; Ali Kakanejadi[a]; Fatemeh Ghenaatian[a]; Zeinab Bigleri[a]
[a] Department of Chemistry, Lorestan University, Khoramabad, Iran

**To cite this Article** Zabardasti, Abedien , Kakanejadi, Ali , Ghenaatian, Fatemeh and Bigleri, Zeinab(2010) 'A theoretical study of cooperative and anticooperative effects on hydrogen-bonded clusters of water and the cyanuric acid', Molecular Simulation, 36: 12, 960 — 968

**To link to this Article: DOI:** 10.1080/08927022.2010.497924

**URL:** http://dx.doi.org/10.1080/08927022.2010.497924

*Molecular Simulation*
Vol. 36, No. 12, October 2010, 960–968

# A theoretical study of cooperative and anticooperative effects on hydrogen-bonded clusters of water and the cyanuric acid

Abedien Zabardasti*, Ali Kakanejadi, Fatemeh Ghenaatian and Zeinab Bigleri

*Department of Chemistry, Lorestan University, Khoramabad, Iran*

(*Received 5 March 2010; final version received 20 May 2010*)

*Ab initio* and density functional calculations are used to analyse the interaction between a molecule of the cyanuric acid and one, two and three molecules of water at B3LYP/6-311 + + G(d,p) and MP2/6-311 + + G(d,p) computational levels. Also, the cooperative effect (CE) in terms of the stabilisation energy of clusters is calculated and discussed. Depending on the geometry of clusters under study, the cooperative, non- or anti-CE was found with an increasing cluster size. Red shifts of N—H and C═O stretching frequencies illustrate a good dependence on the CE. The atoms in molecules theory is used to analyse the CE on topological parameters.

**Keywords:** hydrogen-bonded clusters; cooperative effect; cyanuric acid; theoretical studies; triazinetriol

## 1. Introduction

The cyanuric acid (CA) or 1,3,5-triazine-2,4,6-triol is the cyclic trimer of the cyanic acid [1]. It is an organic chemical compound with the formula $C_3H_3N_3O_3$. Synonyms include 1,3,5-triazinetriol, 1,3,5-triazine-2,4,6(1*H*,3*H*,5*H*)-trione and the isocyanuric acid. This triazine derivative is a stable, white, odourless and hygroscopic solid at room temperature. It is used as a stabiliser in recreational water treatment to minimise the decomposition of the hypochlorous acid by light in outdoor swimming pools and hot tubes [2]. The ring in this molecule has an aromatic character and the hydroxyl (—OH) groups in the triol form of the molecule take on a phenolic character, becoming somewhat more acidic than hydroxyls in an alcohol [3].

Two chemical structures, shown in Scheme 1, are keto–enol tautomers of the CA. Results of theoretical calculations have shown that the keto form is more stable than the enol form [4].

The importance of non-covalent intermolecular interactions in many areas of contemporary chemical physics has been demonstrated in numerous studies of such systems [5]. Non-covalently bonded molecular clusters are of a certain practical importance in many areas such as atmospheric chemistry and catalysis as well as in biochemically relevant processes.

Among all non-covalent interactions, the hydrogen bonding types are particularly significant. Recently, a large number of studies devoted to the hydrogen bonding phenomenon as well as the cooperative effect (CE) in hydrogen-bonded clusters have been published [6–16].

The presence of several alternative hydrogen bond acceptors (HBA, C═O) and hydrogen bond donors (HBD, N—H), which centres on CA, makes it a suitable molecule for the formation of HB clusters.

Despite the potential importance of CA and water, we could find neither experimental nor theoretical report on their H-bond clusters. In the absence of experimental data, a theoretical analysis of such complexes and their properties would appear to be in order. In the present work, a comparative computational study of the molecular properties of $CA(H_2O)n$ ($n = 1–3$) is performed.

## 2. Computational methods

Calculations were performed using the Gaussian 03 system of codes [17]. The geometries of the isolated CA and $H_2O$ molecules and their complexes were fully optimised at B3LYP/6-311 + + G(d,p) and MP2/6-311 + + G(d,p) computational levels. Both MP2 and B3LYP computations have their own supporting instances from the point of agreement between theoretical prediction and experimental measurement [18,19]. Harmonic vibrational frequency calculations at MP2/6-311 ++ G(d,p) and B3LYP/6-311 + + G(d,p) levels confirmed the structures as minima and enabled the evaluation of zero point energy (ZPE). The counterpoise procedure [20] was used to correct the interaction energy for the basis-set superposition error.

## 3. Results and discussion

It seems that adjacent NH···X and CO···Y interactions (X = HBA and Y = HBD) in a cyclic or open Y···O═C—N—H···X form improve each other through both inductive and resonance effects. Clearly, the CO···Y

---

*Corresponding author. Email: zabardasti.a@lu.ac.ir

ISSN 0892-7022 print/ISSN 1029-0435 online

DOI: 10.1080/08927022.2010.497924
http://www.informaworld.com

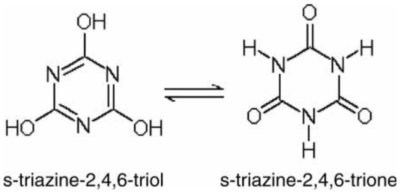

Scheme 1. Enol–keto tautomerisation in the cyanuric acid.

interaction by drawing the electron charge from CO would increase its electron-withdrawing strength on adjacent N atoms. This phenomenon increased the partial positive charges on H atoms of NH groups and gave a stronger NH···X interaction in a charge-assisted hydrogen bond (CAHB) mechanism [21–23]. In contrast, the NH···X interaction would increase the electron donation of N atoms to their adjacent CO, and such an electron donation leads to a stronger CO···Y interaction by increasing the partial negative charges on their O atoms in the CAHB mechanism.

On the other hand, π-bonds of CO groups, which are near to NH with lone pairs of electrons, provide a good path for the resonance-assisted hydrogen bond (RAHB) mechanism [21–23]. Of course, it should be noticed that CAHB and RAHB could act both internally within a Y···O=C—N—H···X unit or externally between separated Y···O=C—N—H···X units in these clusters. It seems that internal CAHB and RAHB mechanisms are more important. Also ability to the formation of bifurcated HB should add to the above subject for some clusters.

The association of one molecule of CA with one molecule of water leads to the formation of a 1:1 complex (S11, Figure 1). The CA molecule acts as both HBD and HBA in the S11 complex.

For 1:2 clusters, starting geometries corresponded to S20, S21, S22 and S23 upon optimisation at MP2 and B3LYP levels (Figure 1). The order of stability of 1:2 clusters was predicted as S20 > S22 > S23 > S21 at both levels. The greater stability of S20 refers to the presence of an additional $H_2O\cdots H_2O$ hydrogen bond, which is absent in other 1:2 clusters. Competition of water molecules for the interaction with the same O atom of the CA in a bifurcated hydrogen bonding leads to the weakest HB interaction in cluster S21 among 1:2 clusters. The interaction of two HBD with an atom as HBA or the interaction of two HBA with an H atom as HBD is anticooperative and give relatively weaker hydrogen-bonded clusters. The greater stability of S22 with respect to S23 might result from a more effective RAHB which can occur in the former. It seems due to shorter distances between HBD and HBA centres of CA, the RAHB process in S22 is more favourable than in S23.

For 1:3 clusters, seven optimised structures have been predicted (Figure 1) whose stabilities are in the order: S30 ≈ S32 > S33 > S31 > S34 > S35 at both MP2 and B3LYP levels.

For the interpretation of these trends, S30 has two $H_2O\cdots H_2O$ bonds, thus the number of its HB is more than other 1:3 clusters, so it was predicted as a more stable 1:3 cluster. On the other hand, stabilities of S31, S32 and S33 with one $H_2O\cdots H_2O$ bond are greater than S34 and S35 which do not have the $H_2O\cdots H_2O$ bond. S34 has three discrete $O\cdots H_2O\cdots HN$ units, which are located on the ring of the CA alternatively. Instead, S35 contains three $O\cdots H_2O\cdots HN$ units with a bifurcated $OH_2\cdots O\cdots H_2O$ bond. The anticooperativity arisen from the $OH_2\cdots O\cdots H_2O$ bond makes S35 the least stable complex among the 1:3 clusters. Similarly, S31, which has one $H_2O\cdots H_2O$ bond, because of a three-centred HB, is less stable than S32 and S33. Stronger HB interactions in S32 relative to S33 result from its better condition for the occurrence of RAHB.

The comparison of data given in Tables 1 and 2 shows that ordering of stabilisation energies (SEs) is the same at the MP2 and B3LYP levels. SEs become more negative by increasing the cluster size. This indicates that an increase in the number of water molecules in the cluster leads to enhanced stability.

Data given in Tables 1 and 2 show that the magnitude of the CE tightly depends on the structure of HB clusters. The CE plays different roles in stability of various clusters. The CE is defined [6] as $\Delta E_{\mathrm{CE}} = \Delta E_{\mathrm{cluster}} - \Sigma\Delta E_{\mathrm{dimer}}$, where the sum is over the 1:1 clusters that make up the given cluster. For example, at the MP2 level, S34 is made up of three S11, which can be written as: $\Delta E_{\mathrm{CE(S34)}} = \mathrm{SE}_{(\mathrm{S34})} - 3 \times \mathrm{SE}_{(\mathrm{S11})} = 0.00\,\mathrm{kcal\,mol^{-1}}$. In other clusters, a combination of a $CO\cdots H_2O$ and a $H_2O\cdots HN$ interactions was taken instead of an S11 cluster.

For instance, in S20: $\Delta E_{\mathrm{CE(S20)}} = \mathrm{SE}_{(\mathrm{S20})} - (\mathrm{SE}_{(\mathrm{S11})} + \mathrm{SE}_{(\mathrm{H_2O\cdots H_2O})}) = -5.61\,\mathrm{kcal\,mol^{-1}}$, the order of cooperativities in 1:2 clusters is in agreement with the predicted order for their stabilities. For S21, S22, S23, S34 and S35, we have small magnitudes for the CE ($\Delta E_{\mathrm{CE}} \approx 0.00$). Hence, on the basis of these results, the CE does not have a significant role in their stabilities. Competition of two water molecules for taking the same lone pair of an O atom of CA in a three-centred H···O···H hydrogen bond does not have a good future for the HB interaction in the S21 cluster. In S22 and S23, we are dealing with two separated $NH\cdots OH_2\cdots O$ units and we could not expect a significant cooperativity in these clusters. By increasing the distance between $NH\cdots OH_2\cdots O$ units on the CA, they will work more independently and the cluster will show an insignificant CE. Greater stabilities of S22 and S32 over S23 and S33, respectively, could be discussed similarly. In contrast, for S20 and S30, we have a chain of hydrogen bonds that could improve each other through a CE.

The order of cooperativities in 1:3 clusters is in line with their stabilities. The 1:3 clusters are more consistent with

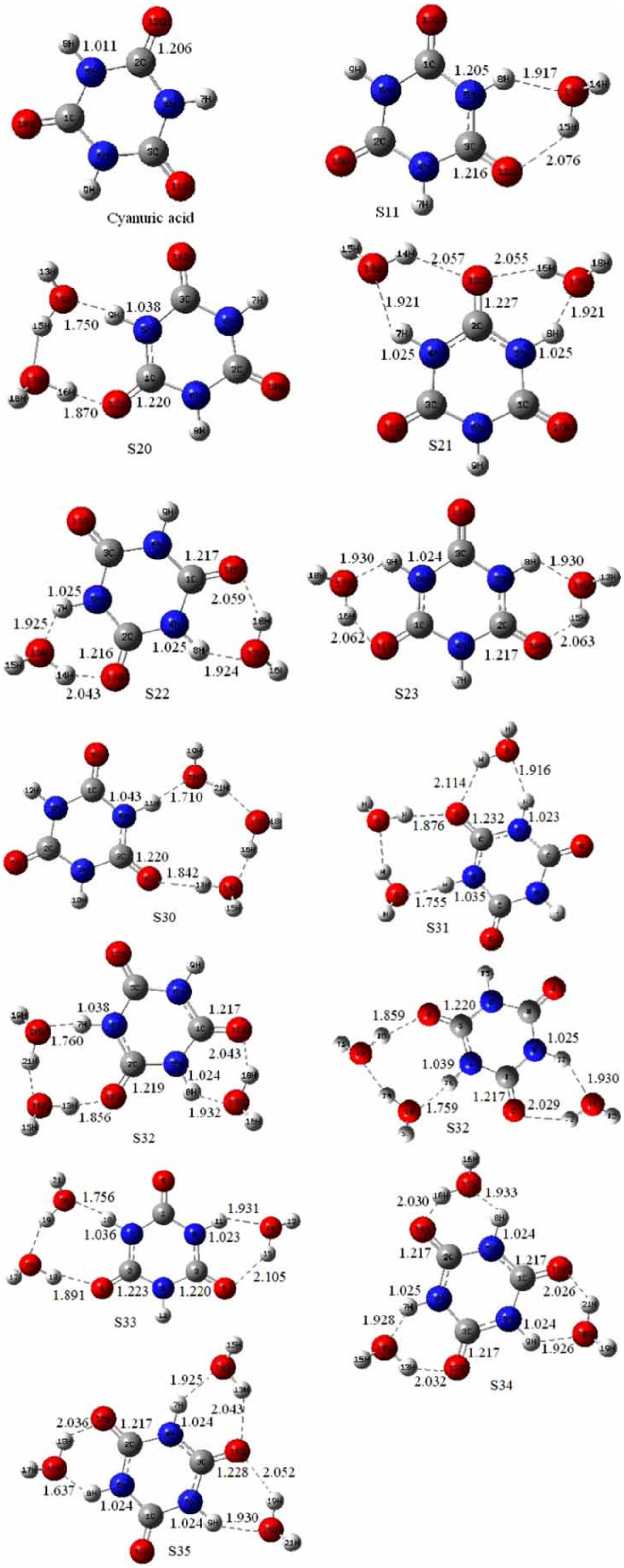

Figure 1. Schematic representation of HB clusters of cyanuric acid and water molecules optimised at MP2/6-311 + + G(d,p).

cooperativity, and values of $\Delta E_{CE}$ are in agreement with SEs in MP2 and B3LYP methods. S35 with $\Delta E_{CE} = 0.57$ and 0.48 in MP2 and B3LYP, respectively, slightly shows an anti-CE with respect to hydrogen bonding.

Also, the CE of 1:2 clusters might be used for the estimation of $\Delta E_{CE}$ of 1:3 clusters. We can consider the cooperativity of S35 as a combination of S21 and S22, then $\Delta E_{CE(S35)} = \Delta E_{CE(S22)} + \Delta E_{CE(S21)} \approx (0.04) + (0.27) = 0.31$, which is close to 0.48 that is obtained by the reported procedure. Of course, since both S21 and S22 are not much favourable clusters in view of cooperativity, low $\Delta E_{CE}$ of S35 is expected. For S34, a similar relationship with S22 could be derived, $\Delta E_{CE(S34)} \approx 2\Delta E_{CE(S22)} = 2 \times (0.04) = 0.08$, which is close to zero that is obtained by the reported procedure. In S31, S32 and S33, because of the contribution of S20 with S21, S22 and S23, respectively, $\Delta E_{CE}$ greater than the estimated values have been obtained. According to the definition which has been employed here, in S35 and S31, due to the presence of anticooperative bifurcated HB, the estimated $\Delta E_{CE}$ from dimers contributed to these clusters are greater than the $\Delta E_{CE}$ calculated by the reported procedure. But in the case of other 1:3 clusters, e.g. S32 and S33, since dimers contributed to the HB cluster are cooperatively positive, $\Delta E_{CE}$ calculated by the reported procedure is greater than the $\Delta E_{CE}$ estimated from discrete dimers contributing to these clusters. The definition is applicable to the estimation of cooperativity and especially the SE of HB clusters of macromolecules and compounds which have a large number of hydrogen bonds.

Some important intra- and intermolecular bond lengths (Å) are given in Figure 1. The N—H and C═O bonds in free CA molecule are 1.013 and 1.211 at the MP2 level. Results given in Figure 1 show lengthening of these bonds upon complex formation. For instance, at the MP2 level, the N—H bond length is 1.024, 1.036, 1.041 Å for S11, S20 and S30, respectively, that has elongated with respect to the free CA molecule. Similarly, for C═O bond, values of 1.219, 1.222 and 1.223 Å were obtained for S11, S20 and S30, respectively, which were greater than 1.211 Å given for free molecules. Similar elongations were predicted at the B3LYP level (Table 3). These greater elongations indicate the stronger HB interactions between CA and $H_2O$ molecules.

Table 1. BSSE, SE corrected with ZPE, uncorrected SE and CE calculated at MP2/6-311 + + G(d,p).

| Cluster | BSSE | $-\mathrm{SE}_{\mathrm{corr}}$ | $-\mathrm{SE}_{\mathrm{unc}}$ | CE |
|---|---|---|---|---|
| S11 | 2.30 | 7.87 | 9.83 | |
| S21 | 4.68 | 15.48 | 19.35 | 0.27 |
| S23 | 4.61 | 15.53 | 19.47 | 0.21 |
| S22 | 4.59 | 15.71 | 19.65 | 0.04 |
| S20 | 5.31 | 17.18 | 21.51 | −5.61 |
| S35 | 7.04 | 23.13 | 29.04 | 0.48 |
| S34 | 6.97 | 23.61 | 29.59 | 0.00 |
| S31 | 7.89 | 24.65 | 31.17 | −5.20 |
| S33 | 7.76 | 25.05 | 31.58 | −5.60 |
| S32 | 7.82 | 25.30 | 31.88 | −5.85 |
| S30 | 8.28 | 25.29 | 32.41 | −10.02 |

Table 2. BSSE, SE corrected with ZPE, uncorrected SE and CE calculated at B3LYP/6-311 + + G(d,p).

| Cluster | BSSE | $-\mathrm{SE}_{\mathrm{corr}}$ | $-\mathrm{SE}_{\mathrm{unc}}$ | CE |
|---|---|---|---|---|
| S11 | 0.85 | 7.12 | 9.11 | |
| S21 | 1.74 | 13.89 | 17.89 | 0.36 |
| S23 | 1.66 | 14.02 | 18.03 | 0.22 |
| S22 | 1.68 | 14.23 | 18.29 | 0.02 |
| S20 | 2.04 | 16.15 | 20.37 | −5.51 |
| S35 | 2.56 | 20.80 | 26.78 | 0.57 |
| S34 | 2.50 | 21.41 | 27.45 | −0.04 |
| S31 | 3.03 | 22.66 | 29.19 | −4.90 |
| S33 | 2.96 | 23.21 | 29.70 | −5.44 |
| S32 | 2.97 | 23.42 | 30.00 | −5.66 |
| S32 | 2.97 | 23.44 | 30.00 | −5.68 |
| S30 | 3.23 | 24.10 | 30.85 | −9.94 |

Results of intermolecular bond lengths are given in Figure 1 and Table 3. The water molecules bind to CA through the NH···O and CO···H hydrogen bond simultaneously. For each cluster, an O···H—N—C═O···H could be considered as a unit of the hydrogen bond. In this unit, the CA acts both as HBD and HBA in the NH···O and CO···H bond, respectively.

The comparison of the NH···O and CO···H bond length in optimised clusters shows that the NH···O interaction is stronger than CO···H. For instance, NH···O bond distances are 1.917, 1.750 and 1.710 Å, while CO···H bond distances are 2.076, 1.870 and 1.842 Å in S11, S20 and S30 clusters, respectively. These results show that for each cluster, the NH···O bond is shorter than the corresponding CO···H bond. Therefore, the former bond is stronger than the latter one.

On the other hand, structures such as S11, S20 and S30 are homologue since their difference is in the number of water molecules in a chain. Results show that in homologue structures, lengths of the NH···O and CO···H bonds decrease by increasing the cluster size. The decrease in these bond distances are consistent with the CEs and is a consequence of the greater stability of higher clusters. Elongation of the C═O bond involved in bifurcated HB is more considerable than C═O bonds contributing to the simple HB. Also, lengthening of bifurcated C═O increases by increasing the cluster size. For example, in S21, S35 and S31, we found values of 1.227, 1.228 and 1.232 Å for this bond.

An interesting subject infers from bond distances given in Figure 1. Comparing the NH···O and CO···H bonds in S11, S22, S23 and S34, which have discrete O···H—N—C═O···H units, shows that these bonds

Table 3. Some selected bond lengths (Å) of hydrogen-bonded clusters.

| Cluster | MP2/6-311++G(d,p) | | | | B3LYP/6-311++G(d,p) | | | |
|---|---|---|---|---|---|---|---|---|
| | $r_{H—N}$ | $r_{NH\cdots O}$ | $r_{C=O}$ | $r_{CO\cdots H}$ | $r_{H—N}$ | $r_{NH\cdots O}$ | $r_{C=O}$ | $r_{CO\cdots H}$ |
| CA | 1.013 | – | 1.211 | – | 1.011 | – | 1.206 | – |
| S11 | 1.024 | 1.911 | 1.219 | 2.147 | 1.025 | 1.916 | 1.216 | 2.076 |
| S20 | 1.035 | 1.748 | 1.222 | 1.904 | 1.038 | 1.750 | 1.220 | 1.870 |
| S21 | 1.024 | 1.919 | 1.228 | 2.106 | 1.025 | 1.921 | 1.227 | 2.055 |
| | 1.024 | 1.917 | 1.228 | 2.105 | 1.025 | 1.921 | 1.227 | 2.057 |
| S22 | 1.023 | 1.925 | 1.219 | 2.097 | 1.025 | 1.925 | 1.216 | 2.043 |
| | 1.023 | 1.922 | 1.219 | 2.113 | 1.025 | 1.924 | 1.217 | 2.059 |
| S23 | 1.023 | 1.924 | 1.220 | 2.116 | 1.024 | 1.931 | 1.217 | 2.060 |
| | 1.023 | 1.924 | 1.220 | 2.117 | 1.024 | 1.932 | 1.217 | 2.060 |
| S30 | 1.041 | 1.702 | 1.223 | 1.857 | 1.043 | 1.710 | 1.220 | 1.842 |
| S31 | 1.023 | 1.916 | 1.232 | 2.114 | 1.025 | 1.919 | 1.231 | 2.069 |
| | 1.035 | 1.755 | 1.232 | 1.786 | 1.038 | 1.759 | 1.231 | 1.858 |
| S32 | 1.036 | 1.755 | 1.222 | 1.887 | 1.039 | 1.756 | 1.219 | 1.856 |
| | 1.023 | 1.926 | 1.220 | 2.096 | 1.024 | 1.932 | 1.217 | 2.042 |
| S33 | 1.036 | 1.756 | 1.223 | 1.891 | 1.038 | 1.762 | 1.221 | 1.861 |
| | 1.023 | 1.931 | 1.220 | 2.105 | 1.024 | 1.937 | 1.217 | 2.055 |
| S34 | 1.023 | 1.928 | 1.219 | 2.080 | 1.024 | 1.933 | 1.217 | 2.030 |
| | 1.023 | 1.928 | 1.219 | 2.081 | 1.024 | 1.926 | 1.217 | 2.026 |
| | 1.023 | 1.929 | 1.219 | 2.079 | 1.025 | 1.928 | 1.217 | 2.043 |
| S35 | 1.023 | 1.923 | 1.229 | 2.083 | 1.024 | 1.925 | 1.228 | 2.052 |
| | 1.023 | 1.926 | 1.229 | 2.093 | 1.024 | 1.930 | 1.228 | 2.093 |
| | 1.023 | 1.932 | 1.219 | 2.081 | 1.024 | 1.937 | 1.217 | 2.036 |

remain constant by increasing the cluster size. This subject confirms the absence of a CE in these clusters.

The selected vibrational stretching frequencies ($\mathrm{cm}^{-1}$) with corresponding intensities ($\mathrm{km\,mol}^{-1}$) for clusters along with N—H and C═O frequency shifts in the CA subunit obtained at two levels are given in Tables 4 and 5. Asymmetric (and symmetric) stretching frequencies of the N—H and C═O bonds have appeared at 3644 (3646) $\mathrm{cm}^{-1}$ and 1838 (1848), respectively, in the free CA molecule at the MP2 level. Upon complex formation, the N—H and C═O bonds contributing to HB with water molecules shifted to lower frequencies. The amount of the red shift depends on strength of their HB interactions with $H_2O$ molecules. Red shifts of N—H bonds in clusters, which have higher degrees of CEs, are greater than clusters with low CEs. Among the studied clusters, the greatest red shift occurs in the N—H stretching frequency ($-514$ and $-486\,\mathrm{cm}^{-1}$ at MP2 and B3LYP levels, respectively) in S30. These red shifts along with values $-415$ and $-465\,\mathrm{cm}^{-1}$ for S20 from 1:2 clusters give further evidence of significance of CEs on stabilities of these clusters. For the following S32, S33 and S31, S30 have larger red shifts for N—H bonds; their order of red shifts are in agreement with the degree of CEs and stabilities of these clusters.

Although NH participated only in simple NH···O hydrogen bonds, CO involved in both simple and bifurcated HBs. Therefore, we should expect a different

Table 4. Unscaled vibrational frequencies ($\mathrm{cm}^{-1}$) with corresponding intensities (values given in parenthesis, $\mathrm{km\,mol}^{-1}$) for the CA molecule in HB clusters calculated at the MP2/6-311 + + G(d, p) level.

| Cluster | $\nu_{NH}$ | $\nu_{C=O}$ | $\Delta\nu_{N—H}$ | $\Delta\nu_{C=O}$ |
|---|---|---|---|---|
| CA | 3644(159)asym, 3646(12)sym | 1838(1045)asym, 1848(10)sym | | |
| S11 | 3449(523) | 1820(835) | −195 | −18 |
| S20 | 3229(1133) | 1814(821) | −415 | −24 |
| S21 | 3450(578), 3457(432) | 1800(702) | −194 | −38 |
| S22 | 3452(744) | 1820(582) | −192 | −18 |
| S23 | 3453(894) | 1816(1114) | −191 | −22 |
| S30 | 3130(1454) | 1808(845) | −514 | −30 |
| S31 | 3226(1138), 3453(495) | 1791(710) | −418 | −47 |
| S32 | 3219(1177), 3461(474) | 1813(828), 1819(705) | −425 | −25 |
| S33 | 3222(1175), 3462(476) | 1811(1024), 1820(516) | −422 | −27 |
| S34 | 3456(732) | 1819(1050) | −188 | −19 |
| S35 | 3456(549), 3466(15) | 1799(707), 1819(709) | −188 | −39 |

Table 5. Unscaled vibrational frequencies ($\mathrm{cm}^{-1}$) with corresponding intensities (values given in parenthesis, $\mathrm{km\,mol}^{-1}$) for the CA molecule in HB clusters calculated at the B3LYP/6-311 + + G(d, p) level.

| Cluster | $\nu_{\mathrm{NH}}$ | $\nu_{\mathrm{C=O}}$ | $\Delta\nu_{\mathrm{NH}}$ | $\Delta\nu_{\mathrm{C=O}}$ |
|---|---|---|---|---|
| CA | 3619(160) | 1814(1095) | | |
| S11 | 3384(553) | 1790(932) | −163 | −24 |
| S20 | 3154(1196) | 1782(935) | −465 | −32 |
| S21 | 3381(603), 3391(487) | 1767(749) | −238 | −47 |
| S22 | 3384(812), 3394(271) | 1789(1100), 1794(615) | −235 | −25 |
| S23 | 3399(94), 3389(974) | 1785(1144), 1796(581) | −220 | −29 |
| S30 | 3061(1561) | 1780(970) | −486 | −6 |
| S31 | 3137(1225), 3386(530) | 1758(737) | −393 | −23 |
| S32 | 3133(1265), 3397(505) | 1782(1006), 1791(704) | −400 | −1 |
| S33 | 3136(1264), 3400(506) | 1779(1119), 1793(614) | −397 | −15 |
| S34 | 3387(795), 3392(718), 3405(85) | 1788(1063), 1789(1054) | −163 | +5 |
| S35 | 3391(577), 3393(999) | 1767(781), 1791(734) | −235 | −3 |

situation for two types of CO with different environments. So, it was cited in the last paragraph about the elongation of the C=O bond; clusters with bifurcated HB (S21, S31 and S35) show larger red shifts for the C=O bond. Data given in Tables 4 and 5 show that for red shifts of C=O bonds, bifurcated HB acts more effectively than the CE.

On the other hand, in systems with discrete O···H—N—C=O···H units (S11, S22, S23 and S34), red shifts of the N—H and C=O bonds are in the same magnitude. It might be considered as a reason for the lack of CEs in such clusters.

The stretching frequencies of O···HN and CO···H bonds (Table 6) show that the former bond appeared in higher frequencies which returns to stronger O···HN interactions. Stretching frequencies of these bonds often increased by increasing the cluster stability.

The atoms in molecules (AIM) theory [24,25] is applied here to analyse the characteristics of the NH···O and H···OC bond critical points (BCP) appearing in studied clusters (Figure 2). The parameters ($\nabla^2_{\rho\mathrm{BCP}}$ is Laplacian of electron density at BCP, $H_{\mathrm{C}}$ is the electron density at BCP and is the sum of the kinetic electron energy density ($G_{\mathrm{C}}$) and the potential electron density ($V_{\mathrm{C}}$)) derived from the Bader theory also indicate the type of interaction and CE on the nature of interactions. The negative value of the Laplacian of the electron density at BCP ($\nabla^2_{\rho\mathrm{BCP}} < 0$) designates the concentration of the electron charge in the region between the nuclei of the interacting atoms and is typical of covalent bonds (shared interactions). In the case of the $\nabla^2_{\rho\mathrm{BCP}} > 0$, there is a depletion of the electron charge between the atoms, which indicates that this is an interaction of closed-shell systems: ions, van der Waals interactions or H-bonds. Hence, one can see that the Bader theory arbitrarily provides the characteristics of BCPs depending on whether the interaction is covalent in nature. For a negative value of a Laplacian, there is no doubt of its covalency (from the AIM theory point of view). Also, the ($-G_{\mathrm{C}}/V_{\mathrm{C}}$) ratio may show the regions belonging to covalent or non-covalent interactions. If such a ratio is greater than 1, then the interaction is non-covalent. In the case of the ratio between 0.5 and 1, the interaction is partly covalent in nature and where ($-G_{\mathrm{C}}/V_{\mathrm{C}}$) is less than 0.5, the interaction is a shared interaction because of $\nabla^2_{\rho\mathrm{BCP}} < 0$ [24].

Table 6. Unscaled vibrational frequencies ($\mathrm{cm}^{-1}$) with corresponding intensities (values given in parenthesis, $\mathrm{km\,mol}^{-1}$) for NH···O and CO···H bonds in HB clusters.

| | MP2/6-311++G(d,p) | | B3LYP/6-311++G(d,p) | |
|---|---|---|---|---|
| Cluster | $\nu_{\mathrm{NH\cdots O}}$ | $\nu_{\mathrm{CO\cdots H}}$ | $\nu_{\mathrm{NH\cdots O}}$ | $\nu_{\mathrm{CO\cdots H}}$ |
| S11 | 97(16) | – | 167(38) | 108(13) |
| S20 | 184(9) | 138(9) | 184(10) | 158(30) |
| S21 | – | 104(42)86(6) | 172(19) | 118(35) |
| S22 | 119(7) | 81(20) | 174(52) | 129(7) |
| S23 | 110(36) | 87(7) | 174(88) | 122(33) |
| S30 | 181(9) | 131(5) | 171(12) | 147(7) |
| S31 | 181(10) | 160(15) 98(15) | 152(23),184(7) | 107(14) |
| S32 | 181(15) | 165(8) 101(13) | 167(8),182(54) | 110(12),164(26) |
| S33 | 182(9)167(12) | 138(10)104(12) | 169(5),181(74) | 113(13),145(24) |
| S34 | 173(5) | 83(21) | 174(25) | 167(24) |
| S35 | 123(35) | 83(23) | 159(11),170(23),171(62) | 134(32) |

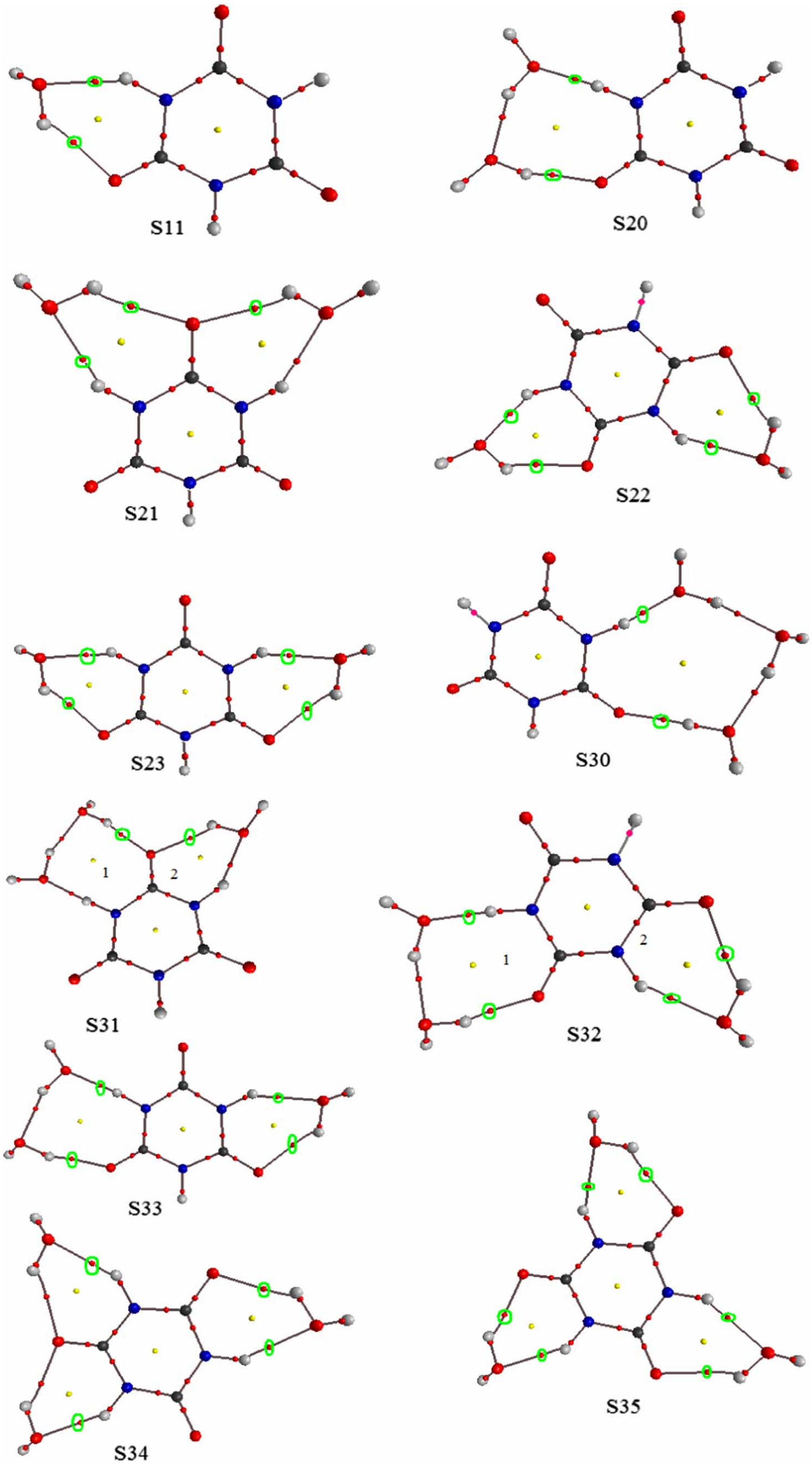

Figure 2. Molecular graphs of fully optimised clusters analysed at the MP2/6-311 + + G(d,p) level.

Table 7. Topological parameters for the optimised systems analysed at the MP2/6-311 + + G(d,p) level.

| NH···O | | | | | | CO···H | | | |
|---|---|---|---|---|---|---|---|---|---|
| Cluster | | $\rho_{BCP}$ | $\nabla^2_\rho$ | $-G_C/V_C$ | $H_C$ | $\rho_{BCP}$ | $\nabla^2_\rho$ | $-G_C/V_C$ | $H_C$ |
| S11 | | 0.0261 | 0.1003 | 1.0910 | −0.0019 | 0.0177 | 0.0648 | 1.1207 | −0.0016 |
| S21 | 1 | 0.0260 | 0.0996 | 1.0919 | −0.0019 | 0.0185 | 0.0678 | 1.1109 | −0.0015 |
| | 2 | 0.0258 | 0.0990 | 1.0926 | −0.0019 | 0.0185 | 0.0675 | 1.1092 | −0.0015 |
| S23 | 1 | 0.0255 | 0.0981 | 1.0978 | −0.0020 | 0.0182 | 0.0666 | 1.1187 | −0.0016 |
| | 2 | 0.0255 | 0.0981 | 1.0980 | −0.0020 | 0.0182 | 0.0666 | 1.1187 | −0.0016 |
| S22 | 1 | 0.0255 | 0.0980 | 1.0969 | −0.0020 | 0.0188 | 0.0687 | 1.1143 | −0.0016 |
| | 2 | 0.0257 | 0.0988 | 1.0951 | −0.0020 | 0.0182 | 0.0666 | 1.1182 | −0.0016 |
| S20 | | 0.0387 | 0.1282 | 0.9452 | 0.0020 | 0.0246 | 0.0990 | 1.1190 | −0.0024 |
| S35 | 1 | 0.0256 | 0.0987 | 1.0971 | −0.0020 | 0.0193 | 0.0176 | 1.1069 | −0.0016 |
| | 2 | 0.0255 | 0.0982 | 1.0980 | −0.0020 | 0.0190 | 0.0694 | 1.1085 | −0.0015 |
| | 3 | 0.0251 | 0.0970 | 1.1016 | −0.0021 | 0.0193 | 0.0707 | 1.1136 | −0.0016 |
| S34 | 1 | 0.0253 | 0.0975 | 1.1006 | −0.0020 | 0.0194 | 0.0711 | 1.1132 | −0.0016 |
| | 2 | 0.0253 | 0.0976 | 1.1005 | −0.0020 | 0.0193 | 0.0710 | 1.1133 | −0.0016 |
| | 3 | 0.0253 | 0.0977 | 1.1004 | −0.0020 | 0.0193 | 0.0708 | 1.1136 | −0.0016 |
| S31 | 1 | 0.0384 | 0.1251 | 0.9435 | 0.0020 | 0.0267 | 0.1052 | 1.0896 | −0.0020 |
| | 2 | 0.0260 | 0.0994 | 1.0903 | −0.0019 | 0.0183 | 0.0665 | 1.1072 | −0.0015 |
| S33 | 1 | 0.0384 | 0.1249 | 0.9437 | 0.0020 | 0.0255 | 0.0255 | 1.1070 | −0.0022 |
| | 2 | 0.0252 | 0.0971 | 1.1001 | −0.0020 | 0.0184 | 0.0674 | 1.1177 | −0.0016 |
| S32 | 1 | 0.0385 | 0.1251 | 0.9428 | 0.0020 | 0.0257 | 0.1028 | 1.1058 | −0.0022 |
| | 2 | 0.0254 | 0.0981 | 1.0985 | −0.0020 | 0.0187 | 0.0685 | 1.1162 | −0.0016 |
| S30 | | 0.0439 | 0.1358 | 0.8989 | 0.0043 | 0.0266 | 0.1089 | 1.1028 | −0.0023 |

The values of topological parameters for each intermolecular BCP of clusters are given in Table 7. According to the criteria mentioned above, the CO···H interactions in all studied clusters are non-covalent ($\nabla^2_{\rho BCP} > 0$, $-G_C/V_C > 1$ and $H_C < 0$), so the CE did not change the identity of these interactions.

Concerning NH···O bonds, there is a tolerance in nature of its interaction with the size and geometry of clusters. For instance, in S20, S30, S31(1), S32(1) and S33(1), this interaction will be partly covalent ($\nabla^2_{\rho BCP} > 0$, $-G_C/V_C < 1$ and $H_C > 0$) and greater covalent character was found in S30 with the smallest value for the $-G_C/V_C$ ratio. But in other clusters this interaction is non-covalent ($\nabla^2_{\rho\,BCP} > 0$, and $-G_C/V_C > 1$).

## 4. Concluding remarks

The mixed clusters of $H_2O$ and CA exhibit a clear evidence of CEs of hydrogen bonding. The present work reports a comparison between the structural, electronic and vibrational properties of complexes of the type $CA(H_2O)_n$ ($n = 1-3$). The general trend is greater SEs along with a smaller hydrogen bond length with increasing cluster size. Cooperative, non-cooperative and anti-CEs might occur in various isomers of a cluster.

## Acknowledgements

We are very grateful to Dr Mahmood Reza Moradian from the English Department of Lorestan University for reading and corrections of this article.

## References

[1] N. Kriebizsch, N.V. Degussa-Antwerpen, H. Klenk, and W.H. Degussa, *Cyanuric acid and cyanuric chloride*, in *Ullmann's Encyclopedia of Industrial Chemistry*, W. Gerhartz, Y.S. Yamamoto, L. Kaudy, R. Pfefferkorn, and F. Rounsavaille, eds., 5th ed., Vol. 8, VCH, New York, 1987, p. 191.

[2] G. Herzberg and C.I. Reid, *Infra-red spectrum and structure of the HNCO molecule*, Discuss. Faraday Soc. 9 (1950), p. 92.

[3] P.G. Maiella and T.B. Brill, *Spectroscopy of hydrothermal reactions III: The water–gas reaction, hot spots and formation of volatile salts of $NCO^-$ from aqueous $[NH_3(CH_2)_nNH_3]NO_3$ (n=2,3) at 720 K and 276 bar by T-Jump/FT-IR spectroscopy*, Appl. Spectrosc. 50 (1996), pp. 829–835.

[4] A. Zabardasti, *Theoretical calculation of equilibrium constant for keto–enol tautomerism in cyanuric acid*, Chem. Heterocycl. Compd. 43 (2007), pp. 1344–1345.

[5] K. Muller-Dethlefs and P. Hobza, *Noncovalent interactions: A challenge for experiment and theory*, Chem. Rev. 100 (2000), pp. 143–168.

[6] S. Scheiner, *Hydrogen Bonding – A Theoretical Perspective*, Oxford University Press, Oxford, 1997.

[7] P. Hobza and Z. Havlas, *Blue-shifting hydrogen bonds*, Chem. Rev. 100 (2000), pp. 4253–4264.

[8] A. Zabardasti, A. Kakanejadifard, and M. Salehnassaj, *Theoretical study of hydrogen bonded clusters of water and isofulminic acid*, J. Theor. Comput. Chem. 8 (2009), pp. 333–345.

[9] A. Zabardasti, S. Amani, M. Solimannejad, and M. Salehnassaj, *Theoretical study and atoms in molecule analysis of hydrogen bonded clusters of ammonia and isocyanic acid*, Struct. Chem. 20 (2009), pp. 1087–1092.

[10] A. Zabardasti and A. Kakanejadifard, *Theoretical study of hydrogen bonded clusters of water and cyanic acid: Hydrogen bonding in terms of the molecular structure*, Polyhedron 27 (2008), pp. 2973–2977.

[11] R.D. Parra and J. Ohlssen, *Cooperativity in intramolecular bifurcated hydrogen bonds: An* ab initio *study*, J. Phys. Chem. A 112 (2008), pp. 3492–3498.

[12] R.D. Parra, M. Furukawa, B. Gong, and X.C. Zeng, *Energetics and cooperativity in three-center hydrogen bonding interactions.*

*I. Diacetamide-X dimers (X=HCN, $CH_3OH$)*, J. Chem. Phys. 115 (2001), pp. 6030–6035.

[13] R.D. Parra, B. Gong, and X.C. Zeng, *Energetics and cooperativity in three-center hydrogen bonding interactions. II. Intramolecular hydrogen bonding systems*, J. Chem. Phys. 115 (2001), pp. 6036–6041.

[14] I. Rozas, I. Alkorta, and J. Elguero, *Bifurcated hydrogen bonds: Three-centered interactions*, J. Phys. Chem. A 102 (1998), pp. 9925–9932.

[15] J. Yang and S.H. Gellman, *Energetic superiority of two-center hydrogen bonding relative to three-center hydrogen bonding in a model system*, J. Am. Chem. Soc. 120 (1998), pp. 9090–9091.

[16] J. Yang, L.A. Christianson, and S.H. Gellman, *Comparison of an HXH three-center hydrogen bond with alternative two-center hydrogen bonds in a model system*, Org. Lett. 1 (1999), pp. 11–14.

[17] M.J. Frisch, G.W. Trucks, H.B. Schlegel, G.E. Scuseria, M.A. Robb, J.R. Cheeseman, J.A. Montgomery, T. Vreven, K.N. Kudin, J.C. Burant, J.M. Millam, S.S. Iyengar, J. Tomasi, V. Barone, B. Mennucci, M. Cossi, G. Scalmani, N. Rega, G.A. Petersson, H. Nakatsuji, M. Hada, M. Ehara, K. Toyota, R. Fukuda, J. Hasegawa, M. Ishida, T. Nakajima, Y. Honda, O. Kitao, H. Nakai, M. Klene, J.E. Knox, H.P. Hratchian, J.B. Cross, C. Adamo, J. Jaramillo, R. Gomperts, R.E. Stratmann, O. Yazyev, A.J. Austin, R. Cammi, C. Pomelli, J.W. Ochterski, P.Y. Ayala, K. Morokuma, G.A. Voth, P. Salvador, J.J. Dannenberg, V.G. Zakrzewski, S. Dapprich, A.D. Daniels, M.C. Strain, O. Farkas, D.K. Malick, A.D. Rabuck, K. Raghavachari, J.B. Foresman, J.V. Ortiz, Q.Cui, A.G. Baboul, S. Clifford, J. Cioslowski, B.B. Stefanov, G. Liu, A. Liashenko, P. Piskorz, I. Komaromi, R.L. Martin, D.J. Fox, T. Keith, M.A. Al-Laham, C.Y. Peng, A. Nanayakkara, M. Challacombe, P.M.W. Gill, B. Johnson, W. Chen, M.W. Wong, C. Gonzalez, and J.A. Pople, *Gaussian 03*, *Revision B.05*, Gaussian Inc., Pittsburgh, PA, 2003.

[18] P. Hobza, V. Spirko, Z. Havlas, K. Buchhold, B. Reimann, H.D. Barth, and B. Brutschy, *Anti-hydrogen bond between chloroform and fluorobenzene*, Chem. Phys. Lett. 299 (1999), pp. 180–186.

[19] H. Matsuura, H. Yoshida, M. Hieda, S. Yamanaka, T. Harada, K. Shin-ya, and K. Ohno, *Experimental evidence for intramolecular blue-shifting C—H···O hydrogen bonding by matrix-isolation infrared spectroscopy*, J. Am. Chem. Soc. 125 (2003), pp. 13910–13911.

[20] S.F. Boys and F. Bernardi, *The calculation of small molecular interactions by the differences of separate total energies. Some procedures with reduced errors*, Mol. Phys. 19 (1970), p. 553.

[21] J.N. Woodford, *Density functional theory and atoms-in-molecules investigation of intramolecular hydrogen bonding in derivatives of malonaldehyde and implications for resonance-assisted hydrogen bonding*, J. Phys. Chem. A 111 (2007), pp. 8519–8530.

[22] S.J. Grabowski, W.A. Sokalski, and J. Leszczynski, *How short can the H···H intermolecular contact be? New findings that reveal the covalent nature of extremely strong interactions*, J. Phys. Chem. A 109 (2005), pp. 4331–4341.

[23] M. Ziółkowski, S.J. Grabowski, and J. Leszczynski, *Cooperativity in hydrogen-bonded interactions:* Ab initio *and atoms in molecules analyses*, J. Phys. Chem. A 110 (2006), pp. 6514–6521.

[24] R.F.W. Bader, *Atoms in Molecules: A Quantum Theory*, Oxford University Press, Oxford, UK, 1990.

[25] P.L.A. Popelier, *Atoms in Molecules, an Introduction*, Prentice Hall. Upper Saddle River, NJ, 2000.